

Photochemical & Photobiological Sciences

Accepted Manuscript



This is an *Accepted Manuscript*, which has been through the Royal Society of Chemistry peer review process and has been accepted for publication.

Accepted Manuscripts are published online shortly after acceptance, before technical editing, formatting and proof reading. Using this free service, authors can make their results available to the community, in citable form, before we publish the edited article. We will replace this *Accepted Manuscript* with the edited and formatted *Advance Article* as soon as it is available.

You can find more information about *Accepted Manuscripts* in the [Information for Authors](#).

Please note that technical editing may introduce minor changes to the text and/or graphics, which may alter content. The journal's standard [Terms & Conditions](#) and the [Ethical guidelines](#) still apply. In no event shall the Royal Society of Chemistry be held responsible for any errors or omissions in this *Accepted Manuscript* or any consequences arising from the use of any information it contains.

Enhanced upconversion Luminescence through core/shell structures and its application for detecting organic dyes in opaque fishes

Pan Hu,^a Xiaofeng Wu,^{*a} Shigang Hu,^a Zenghui Chen,^b Huanyuan Yan,^c Zaifang Xi,^a Yi Yu,^a Gangtao Dai,^b and Yunxin Liu^{*b,d}

^aSchool of Information and Electrical Engineering, ^bDepartment of Physics and Electrical Science, ^cCollege of Mechanical and Electrical Engineering, Hunan University of Science and Technology, Xiangtan 411201, china.

^dINPAC-Institute for Nanoscale Physics and Chemistry, KU Leuven, Celestijnenlaan 200D B-3001, Belgium.

Abstract: Here, we report the enhanced upconversion luminescence of NaLuF₄:18%Yb³⁺,2%Er³⁺ through core/shell structures. Among NaYF₄, NaGdF₄, and NaLuF₄ shells, the first one presents the highest efficiency. These upconversion fluorescent nanoprobe with oleic acid/PEG hybrid ligand can efficiently capture Rhodamine B (RB) and sodium fluorescein (SF) in opaque fishes to present their residues in vivo through luminescence resonant energy transfer (LRET) processes. It can be addressed based on LRET technology that no RB is absorbed by opaque fishes after incubating in the aqueous solution of 1 µg/ml RB for one day, while SF residue can be obviously detected after incubating in the aqueous solution of 1 µg/ml SF for one day. The merit of this LRET technology with upconversion nanoparticle (UCNP) donor is ascribed to the deep penetration depth of infrared pumping laser and high signal to noise ratio.

Keywords: LRET; upconversion luminescence; biophysical sensors; fluorescent dyes; nanoprobe.

Organic dyes are widely used in textile and printing industries which are one of the largest groups of pollutants released into waste water [1-3]. Most of organic dyes are toxic to aquatic organisms, animals, as well as human beings [4-5]. It is very urgent to develop efficient methods for detecting traces of organic dyes in living things and thus supplying the toxicity analysis with direct information [6-7]. The rapid and

precise detection of organic dyes will help human beings from the harm of toxic dyes [8]. Up to now, a variety of methods have been developed for detecting organic dyes based on fluorescence resonant energy transfer (FRET) technology [9]. The key for FRET spectra detection or imaging is to select an efficient and stable fluorescence donor. Usually, quantum dots (QDs) [10], fluorescent proteins

[11-12], or fluorescent organic compounds [13], are used as fluorescence donors. However, the intrinsic drawbacks of these donors, e.g. poor stability and low signal to noise ratio under the pumping of ultraviolet light, limit their application for high precision detecting of organic dyes and hinder their development in the field of clinical medicine [14-18]. Furthermore, expensive pulse lasers are need for exciting the fluorescent proteins or quantum dots to meet the high power densities requirement to observe the two-photon effect [19-21].

Upconversion nanoparticles have recently received extensive and increasing attention which can convert low energy infrared photons to higher energy visible photons. Because of sharp emission band, superior photostability, deep tissue penetration of near-infrared excitation, and background-free fluorescent imaging, upconversion nanoparticles are ideal candidates for substituting the conventional donors in FRET technology [22-25].

In our previous works [26-27], we have applied upconversion nanoparticles as fluorescence donors to detecting organic dyes in plant cells and transparent jellyfish, and obtained high detection precision. Here, we present the in vivo detection of organic dyes in opaque fishes through LRET from upconversion nanoparticles to dyes. It is rapidly addressed based on LRET technology that no RB is absorbed by the opaque fishes after incubating in the aqueous solution of 1 $\mu\text{g}/\text{ml}$ RB for one day, while SF residue can be obviously detected after incubating in the aqueous solution of 1 $\mu\text{g}/\text{ml}$ SF for one day.

Upconversion nanoparticles were

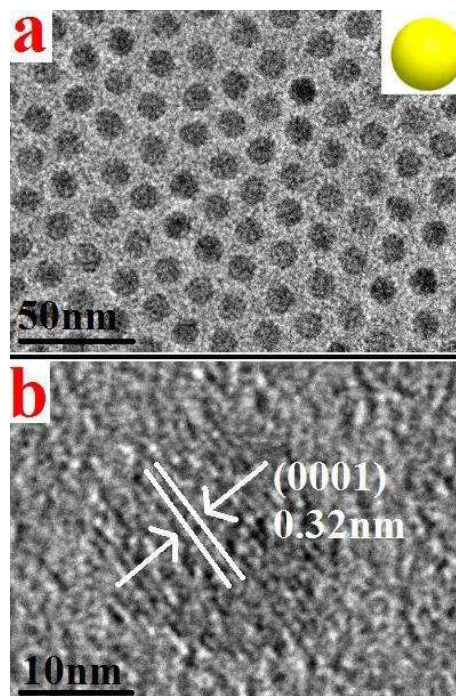


Fig. 1. TEM images of (a) $\text{NaLuF}_4:18\%\text{Yb}^{3+},2\%\text{Er}^{3+}$ core NPs. Inset: the model of a single core nanoparticle; (b) the corresponding high-resolution TEM images (HR-TEM).

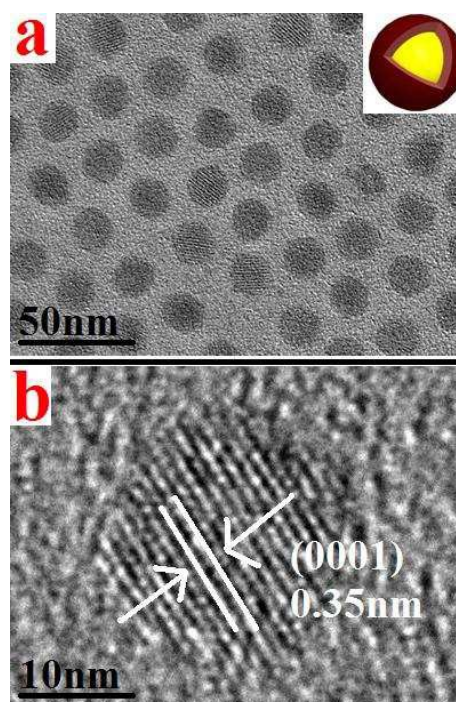


Fig. 2. TEM images of (a) $\text{NaLuF}_4:18\%\text{Yb}^{3+},2\%\text{Er}^{3+}/\text{NaGdF}_4$ core/shell NPs. Inset: the model of a single core/shell nanoparticle; (b) the corresponding high-resolution TEM images (HR-TEM).

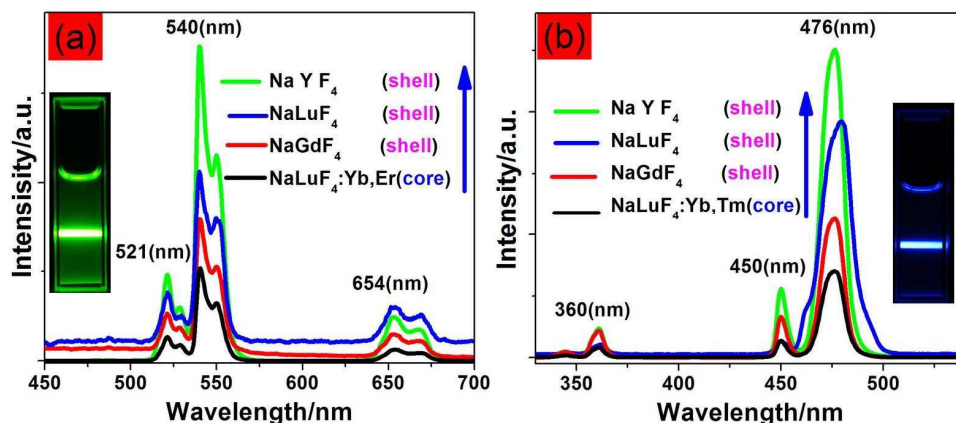


Fig. 3. Room temperature upconversion emission spectra of (a) $\text{NaLuF}_4:18\%\text{Yb}^{3+},2\%\text{Er}^{3+}$ core and $\text{NaLuF}_4:18\%\text{Yb}^{3+},2\%\text{Er}^{3+}/\text{NaLnF}_4$ ($\text{Ln}=\text{Y}, \text{Lu}, \text{Gd}$) core/shell nanoparticles; (b) $\text{NaLuF}_4:18\%\text{Yb}^{3+},0.5\%\text{Tm}^{3+}$ core and $\text{NaLuF}_4:18\%\text{Yb}^{3+},0.5\%\text{Tm}^{3+}/\text{NaLnF}_4$ ($\text{Ln}=\text{Y}, \text{Lu}, \text{Gd}$) core/shell nanoparticles.

synthesized by our previous route [28] (Details listed in Supporting Information). The photoluminescence emission spectra was measured from 400 to 700 nm using a Hitachi F-2700 spectrophotometer equipped with a 980 nm laser as the excitation source.

The photos of upconversion luminescence were obtained digitally by a Nikon camera D3200. $\text{NaLuF}_4:18\%\text{Yb}^{3+},2\%\text{Er}^{3+}$ core and $\text{NaLuF}_4:18\%\text{Yb}^{3+},2\%\text{Er}^{3+}/\text{NaLnF}_4$ ($\text{Ln}=\text{lanthanide}$) core/shell nanoparticles were characterized by TEM and shown in Figure 1 and 2. It is clear from Fig. 1a that $\text{NaLuF}_4:18\%\text{Yb}^{3+},2\%\text{Er}^{3+}$ core nanocrystals have spherical morphology and uniform particle size. Figure 1b shows the good crystallinity of these core nanoparticles. The distances between the lattice fringes were measured to be 0.32 nm along (0001) orientation in the hexagonal NaLuF_4 nanocrystals [29-31]. After coating with a thin shell of NaGdF_4 (Fig. 2a), the overall particle size of $\text{NaLuF}_4:18\%\text{Yb}^{3+},2\%\text{Er}^{3+}$ core nanoparticles increases from 15 nm to 20 nm. It can be seen that the NaGdF_4

shell has also well crystallinity (Fig. 2b).

The upconversion fluorescent spectra of $\text{NaLuF}_4:18\%\text{Yb}^{3+},2\%\text{Er}^{3+}$ core nanocrystals and $\text{NaLuF}_4:18\%\text{Yb}^{3+},2\%\text{Er}^{3+}/\text{NaLnF}_4$ ($\text{Ln}=\text{Y}, \text{Lu}, \text{Gd}$) core/shell nanocrystals in cyclohexane solution under the 980 nm laser excitation are shown in Fig. 3a. It is observed that the integral emission intensity of $\text{NaLuF}_4:18\%\text{Yb}^{3+},2\%\text{Er}^{3+}/\text{NaLnF}_4$ ($\text{Ln}=\text{Y}, \text{Lu}, \text{Gd}$) core/shell NPs is higher than $\text{NaLuF}_4:18\%\text{Yb}^{3+},2\%\text{Er}^{3+}$ core NPs, because the surface defects of $\text{NaLuF}_4:18\%\text{Yb}^{3+},2\%\text{Er}^{3+}$ core NPs were considerably eliminated in the core/shell structures. The similar phenomenon is also observed by comparing the fluorescent spectra of $\text{NaLuF}_4:18\%\text{Yb}^{3+},0.5\%\text{Tm}^{3+}$ core and $\text{NaLuF}_4:18\%\text{Yb}^{3+},0.5\%\text{Tm}^{3+}/\text{NaLnF}_4$ ($\text{Ln}=\text{Y}, \text{Lu}, \text{Gd}$) core/shell NPs (Fig.3b). It is noted that NaYF_4 shell is the most efficient among the three shells for enhancing the upconversion luminescence, since the phonon energy (A' Mode = 211 cm^{-1}) of NaYF_4 host is obvious lower than those for NaLuF_4 (A' Mode > 264 cm^{-1}) and NaGdF_4 (A'

Mode= 293 cm^{-1}) host [32-33]. The low phonon energy of the host directly leads to high photon-upconversion efficiency and low non-radiative cross-relaxation probability. This is also in agreement with the simulation calculation [34], the vibration energy of Gd^{3+} based host is the highest among the three host ions due to the unpaired electrons of Gd^{3+} . In addition, the outmost-shell of Y^{3+} ion has no electron while the outmost 4f-shell of Lu^{3+} ion are fully filled with 14 electrons. As a result, both NaYF_4 and NaLuF_4 shells have no unpaired electron to exchange energy with the emitters Er^{3+} or Tm^{3+} ion in the core particles. But, the outmost shells of Gd^{3+} ions have 7 unpaired electrons so that NaGdF_4 shells can exchange energy with emitters Er^{3+} and Tm^{3+} in the core nanoparticles through the non-radiative cross relaxation [35]. This may be the reason why the NaGdF_4 shells are less efficient than NaLuF_4 shells for enhancing the emission of the core nanoparticles. In comparison to Lu^{3+} (1.27), Y^{3+} (1.22) ion has lower electronegativity, which is the third factor for the highest efficiency of NaYF_4 shell [36]. The above three factors determine that the NaYF_4 shell presents the highest efficiency for improving the emission intensity of core nanoparticles. The emission bands can be easily assigned to the transition within the 4fⁿ shells of the Er^{3+} and Tm^{3+} ions. The spectrum of the $\text{NaLuF}_4:18\%\text{Yb}^{3+},2\%\text{Er}^{3+}$ (Fig.3a) exhibits three distinct emission bands from Er^{3+} ions, centered at 521nm, 540nm, and 654nm which are assigned to the Er^{3+} -4fⁿ electronic transitions ${}^2\text{H}_{11/2} \rightarrow {}^4\text{I}_{15/2}$, ${}^4\text{S}_{3/2} \rightarrow {}^4\text{I}_{15/2}$ and ${}^4\text{F}_{9/2} \rightarrow {}^4\text{I}_{15/2}$, respectively. The whole

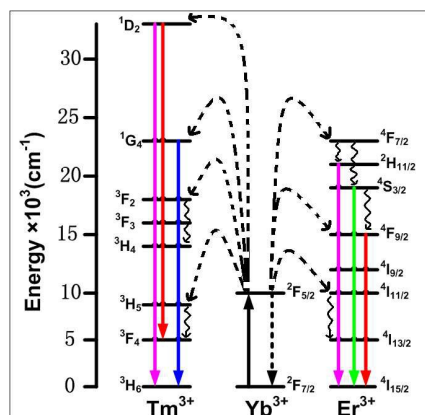


Fig. 4. The energy level diagrams of the Er^{3+} , Tm^{3+} and Yb^{3+} dopant ions and upconversion mechanisms following 980 nm laser diode excitation.

luminescence appears green in color to naked eyes due to the combination of intense green and weak red emissions from the Er^{3+} ion. Three emission bands from the Tm^{3+} were observed in the $\text{NaLuF}_4:18\%\text{Yb}^{3+},0.5\%\text{Tm}^{3+}$ (Fig. 3b) under the 980 nm laser diode excitation. The strongest band centered at 476 nm was assigned to the ${}^1\text{G}_4 \rightarrow {}^3\text{H}_6$ transition of Tm^{3+} ion and another weak blue emission band centered at 450 nm was assigned to the ${}^1\text{D}_2 \rightarrow {}^3\text{F}_4$ transition. Noticeably, an intense near ultraviolet emission band centered at 360 nm was observed which was assigned to the ${}^1\text{D}_2 \rightarrow {}^3\text{H}_6$ transition of Tm^{3+} ions. The overall emission shows blue color to naked eyes since the visible blue emission is much stronger than other emission band.

The possible upconversion excitation emission pathways of the $\text{Er}^{3+}/\text{Yb}^{3+}$ and $\text{Tm}^{3+}/\text{Yb}^{3+}$ ion couples are shown in Fig. 4 [37-41]. In the case of $\text{NaLuF}_4:18\%\text{Yb}^{3+},2\%\text{Er}^{3+}$, an initial energy transfer from an Yb^{3+} ion in the ${}^2\text{F}_{5/2}$ state to an Er^{3+} ion populating the ${}^4\text{I}_{11/2}$ level of Er^{3+} ion. The second 980 nm photon or energy transfer from an Yb^{3+} ion to the Er^{3+} ion can then

populate the $^4F_{7/2}$ level of the Er^{3+} ion. The electrons in the $^4F_{7/2}$ level of Er^{3+} ion can relax nonradiatively (without emission of photons) to the $^4S_{3/2}$ levels for the green emissions by the transition $^4S_{3/2} \rightarrow ^4I_{15/2}$. Alternatively, the Er^{3+} ion can further relax and populate the $^4F_{9/2}$ level leading to the red emission from the transition $^4F_{9/2} \rightarrow ^4I_{15/2}$. The $^4F_{9/2}$ level may also be populated from the $^4I_{13/2}$ level of the Er^{3+} ion by absorption of a 980 nm photon, or energy transfer from an Yb^{3+} ion, with the $^4I_{13/2}$ state being initially populated via the nonradiative $^4I_{11/2} \rightarrow ^4I_{13/2}$ relaxation. For the $NaLuF_4:18\%Yb^{3+},0.5\%Tm^{3+}$, up to three subsequent energy transfers from Yb^{3+} ions to Tm^{3+} to populate the upper Tm^{3+} ions 1G_4 levels for emitting 450 nm and 476 nm blue light. Rhodamine B and Sodium fluorescein are selected as model dyes to explore the residual of organic dyes in opaque fishes. There is a perfect overlap between the excitation spectra of Rhodamine B and the emission spectra of $NaLuF_4:18\%Yb^{3+},2\%Er^{3+}$ nanoparticles in green region, so that an LRET based sensor system can be successfully constructed by combining the UCNP with Rhodamine B, in which UCNP play a role of energy donor while Rhodamine B plays a role of energy acceptor (see Supporting Information Scheme S1b). In addition, oleic acid molecule pairs can form on the surfaces of the upconversion nanoparticles (see Scheme S1a), which compacted with each other through the weak hydrogen-bond interaction. As a result, the carboxyl group of one oleic acid molecule connected to upconversion nanoparticle and the other oleic acid molecule can release one free carboxyl

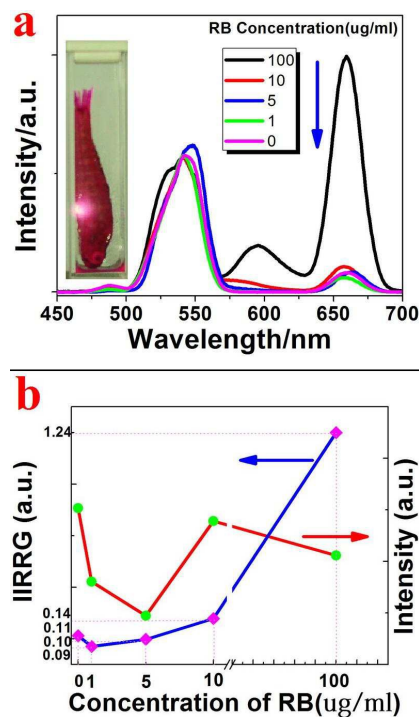


Fig. 5. (a) In vivo upconversion fluorescent spectra of the opaque fishes after cultured in aqueous solution with different concentrations of Rhodamine B for one day using $NaLuF_4:18\%Yb^{3+},2\%Er^{3+}/NaYF_4$ core/shell nanocrystals as probes. Photo: the fluorescence imaging was collected by a Nikon camera D3200 under the excitation of a 980 nm laser diode. (b) Integral Intensity Ratio of red (RB) to green (UCNPs) (IIRRG) vs. concentration of RB; overall fluorescent intensity of UCNPs@RB vs. concentration of RB in opaque fishes.

(see Scheme S1a). These oleic acid molecule pairs are confirmed by the absorption of UCNP to fluorescent dyes. The same phenomenon is much remarkable for SF solution which also is a perfect overlap between the excitation spectra of sodium fluorescein and the emission spectra of $NaLuF_4:18\%Yb^{3+},0.5\%Tm^{3+}$ nanoparticles in blue region (see Scheme S1c).

Conventional detection of organic dyes is restricted to operation in vitro. Here, we show that the green upconversion fluorescent nanoprobe is very efficient and viable for detecting Rhodamine-B in vivo, based on the luminescent resonance energy transfer

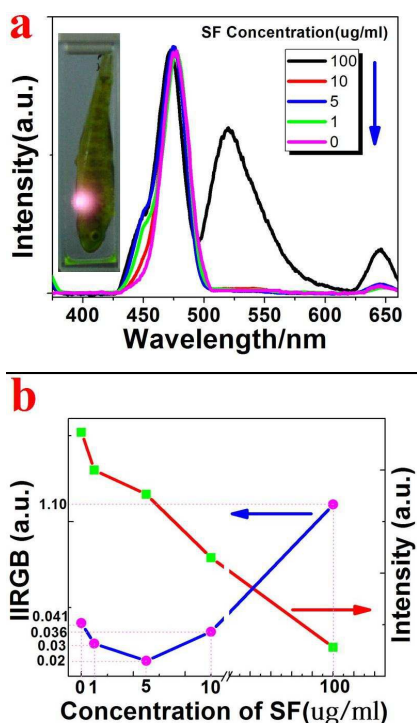


Fig. 6. (a) In vivo upconversion fluorescent spectra of the opaque fishes after cultured in aqueous solution with different concentrations of sodium fluorescein for one day using $\text{NaLuF}_4:18\%\text{Yb}^{3+},05\%\text{Tm}^{3+}/\text{NaYF}_4$ core/shell nanocrystals as probes. Photo: the fluorescence imaging was collected by a Nikon camera D3200 under the excitation of a 980 nm laser diode. (b) Integral Intensity Ratio of green (SF) to blue (UCNPs) (IIRGB) vs. concentration of SF; overall fluorescent intensity of UCNPs@SF vs. concentration of SF in opaque fishes.

process from UCNPs to Rhodamine-B. The main merits of these UCNPs based LRET are ascribed to the deep penetration depth of the infrared excitation light and high signal to noise ratios.

$\text{NaLuF}_4:18\%\text{Yb}^{3+},2\%\text{Er}^{3+}/\text{NaYF}_4$ core/shell nanoparticles were first selected as fluorescent donors for detecting Rhodamine-B in vivo. We injected the opaque fishes with UCNPs (16.5 mg/ml), which have been incubated in aqueous solution of various concentrations of RB for one day, and then a series of LRET spectra were recorded in vivo and shown in Fig. 5a. It is noted that the emission of the fish (in vivo) is slightly different from the case

in solution (Fig.S5), which is due to the fish tissues induced reflection and scattering to the fluorescence. There are three emission peaks in the in vivo fluorescent spectra consistent with RB concentration of 1~100 $\mu\text{g/ml}$ (see Fig. 5a). The green emission band centered at 545 nm and the red emission band centered at 654 nm are ascribed to the 4f-shell electronic transitions $^4\text{S}_{3/2} \rightarrow ^4\text{I}_{15/2}$ and $^4\text{F}_{9/2} \rightarrow ^4\text{I}_{15/2}$ of Er^{3+} , respectively. The yellow emission band centered at 590 nm originates the exciton recombination radiation in Rhodamine-B. It is noted that the yellow emission peak (590 nm) from RB increases relative to the green emission (545 nm) from upconversion nanoparticles with increasing the concentration of RB. It is clear from Fig. 5a that the opaque fish presents yellow light under the excitation of 980 nm infrared light, which are actually composed of the green emission of $\text{NaLuF}_4:18\%\text{Yb}^{3+},2\%\text{Er}^{3+}/\text{NaYF}_4$ core/shell UCNPs and the yellow emission of RB. Meanwhile, it is quite clear from Fig. 5b that the intensity ratio of the emission from RB to that of upconversion nanoparticles increases with increasing the concentration of the dyes, while the overall fluorescent intensity from dyes and upconversion nanoparticles decreases with further increasing the concentration of the dyes higher than 10 $\mu\text{g/ml}$. Combining the LRET spectra of Fig. 5b with Fig. S5, it can be addressed that no RB is absorbed by opaque fishes after incubating in the aqueous solution of 1 $\mu\text{g/ml}$ RB for one day. This indicates that the aqueous solution with RB concentration lower than 1 $\mu\text{g/ml}$ has no obvious influence on the common life of the opaque fishes.

We also investigated residual of sodium fluorescein in the opaque fishes by employing the same procedure. NaLuF₄:18%Yb³⁺,0.5%Tm³⁺/NaYF₄ core/shell blue upconversion nanocrystals were selected as fluorescent donor. The LRET fluorescent spectra of UCNPs@SF system with various concentration of SF were also recorded in vivo and shown in Fig. 6a. There are three emission peaks in the in vivo fluorescent spectra consistent with SF concentration of 1~100 ug/ml (see Fig. 6a). The blue emission band centered at 476 nm and the red emission band centered at 645 nm are ascribed to the 4f-shell electronic transitions ¹G₄→³H₆ and ¹G₄→³F₄ of Tm³⁺, respectively. The green emission band centered at 521 nm originates the exciton recombination radiation in sodium fluorescein. Combining the LRET spectra of Fig. 6b with Fig. S6, it can be addressed that SF residue obviously existed in the opaque fishes and can be rapidly detected after incubating in the aqueous solution of 1 μg/ml SF for one day. This indicates that the aqueous solution with SF concentration higher than 1 μg/ml is not suitable for the common life of the opaque fishes and may lead to the unrecoverable biochemical injury.

In conclusion, the upconversion luminescence of NaLuF₄:18%Yb³⁺,2%Er³⁺ and NaLuF₄:18%Yb³⁺,0.5%Tm³⁺ nanoparticles were enhanced by coating with a thin shell (2.5 nm) of NaLnF₄ (Ln = lanthanide). Among NaYF₄, NaGdF₄ and NaLuF₄ shells, the first one present the highest efficiency for enhancing the upconversion luminescence of NaLuF₄:18%Yb³⁺,2%Er³⁺ core

nanoparticles, which is mainly ascribed to the lowest phonon energy of NaYF₄ host. These upconversion nanoparticles with enhanced luminescence can meet the requirement for detecting fluorescent dyes in opaque fishes, beyond in the transparent opaque fishes [27]. Upconversion nanoprobe with oleic acid/PEG hybrid ligand can efficiently capture Rhodamine B (RB) and sodium fluorescein (SF) in opaque fishes to present their residues in vivo through luminescence resonant energy transfer (LRET) processes. It can be addressed based on LRET technology that no RB is absorbed by the opaque fishes after incubating in the aqueous solution of 1 μg/ml RB for one day, while SF residue can be obviously detected after incubating in the aqueous solution of 1 μg/ml SF for one day.

We expect these results will accelerate the application of LRET technology in opaque living things.

Acknowledgements

Project supported by the National Natural Science Foundation of China (Grant Nos 21301058, 61376076, 61575062 and 11204076); supported by the Scientific Research Fund of Hunan Provincial Education Department (Grant No.14B060) and Natural Science Foundation of Hunan Provincial (Grant No.13JJ4048).

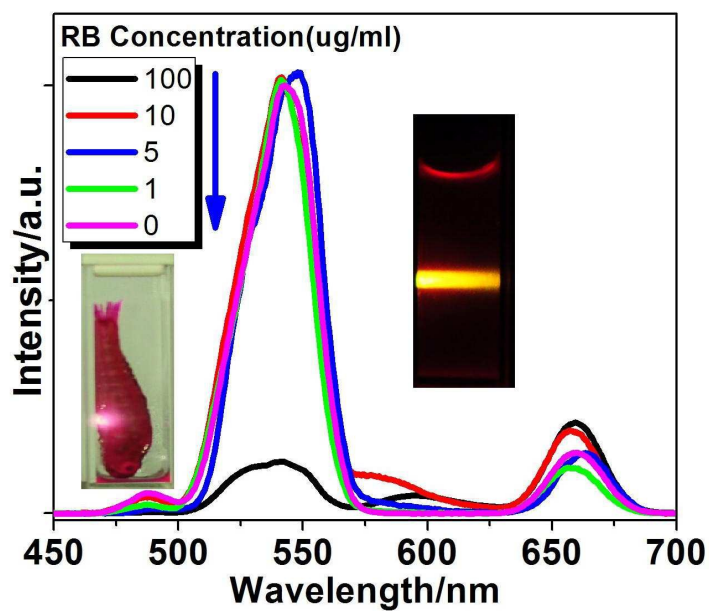
References

- [1] Z. Aksu, Application of biosorption for the removal of organic pollutants: a review Process, *Biochemistry.*, 2005, **40**, 997–1026.
- [2] A. Carlos, M. Huitle and S. G. Ferro, Electrochemical oxidation of organic

- pollutants for the wastewater treatment: direct and indirect processes, *Chem. Soc. Rev.*, 2006, **35**, 1324–1340.
- [3] T. Zhu, J. S. Chen and X. W. Lou, Highly Efficient Removal of Organic Dyes from Waste Water Using Hierarchical NiO Spheres with High Surface Area, *J. Phys. Chem. C.*, 2012, **116**, 6873–6878.
- [4] S. B. Wang, Y. Boyjoo, A. Choueib and Z. H. Zhu, Removal of dyes from aqueous solution using fly ash and red mud, *Water Research.*, 2005, **39**, 129–138.
- [5] F. A. Pavan, S. L. P. Dias, E. C. Lima and E. V. Benvenuti, Removal of Congo red from aqueous solution by anilinepropylsilica xerogel, *Dyes and Pigments.*, 2008, **76**, 64-69.
- [6] Z. A. qodah, Adsorption of dyes using shale oil ash, *Wat. Res.*, 2000, **34**, 4295-4303.
- [7] P. Janos, H. Buchtova and M. Ryznarova, Sorption of dyes from aqueous solutions onto fly ash, *Water Research*, 2003, **37**, 4938–4944.
- [8] W. Tanthapanichakoon, P. Ariyadejwanich, P. Japthong, K. Nakagawa, S. R. Mukai and H. Tamon, Adsorption–desorption characteristics of phenol and reactive dyes from aqueous solution on mesoporous activated carbon prepared from waste tires, *Water Research.*, 2005, **39**, 1347–1353.
- [9] R. G. Ute, M. Grabolle, C. J. Sara, R. Nitschke and T. Nann, Quantum dots versus organic dyes as fluorescent labels, *Nature methods.*, 2008, **5**, 763-775.
- [10] I. L. Medintz, A. R. Clapp, H. Mattoussi, E. R. Goldman, B. Fisher and J. M. Mauro, Self-assembled nanoscale biosensors based on quantum dot FRET donors, *Nature materials.*, 2003, **9**, 630-638.
- [11] M. A. Rizzo, G. H. Springer, B. Granada and D. W. Piston, An improved cyan fluorescent protein variant useful for FRET, *Nature biotechnology.*, 2004, **4**, 445-449.
- [12] A. W. Nguyen and P. S. Daugherty, Evolutionary optimization of fluorescent proteins for intracellular FRET, *Nature biotechnology.*, 2005, **3**, 355-360.
- [13] X. Zhang, Y. Xiao and X. Qian, A ratiometric fluorescent probe based on FRET for imaging Hg²⁺ ions in living cells, *Angewandte Chemie International Edition.*, 2008, **42**, 8025-8029.
- [14] D. Q. Chen, L. Liu, P. Huang, M. Y. Ding, J. S. Zhong and Z. G. Ji, Nd³⁺-Sensitized Ho³⁺ Single-Band Red Upconversion Luminescence in Core-Shell Nanoarchitecture, *J. Phys. Chem. Lett.*, 2015, **6**, 2833-2851.
- [15] C. Warren, W. Chan and S. M. Nie, Quantum Dot Bioconjugates for Ultrasensitive Nonisotopic Detection, *Science.*, 1998, **281**, 2016-2018.
- [16] I. L. Medintz, H. T. Uyeda, E. R. Goldman and H. Mattoussi, Quantum dot bioconjugates for imaging, labelling and sensing, *Nature materials.*, 2005, **4**, 435-446.
- [17] W. C. Chan, D. J Maxwell, X. H. Gao, R. E. Bailey, M. Y. Han and S. M. Nie, Luminescent quantum dots for multiplexed biological detection and imaging, *Current Opinion in Biotechnology.*, 2002, **13**, 40–46.

- [18] B. Dubertret, P. Skourides, D. J. Norris, V. Noireaux, A. H. Brivanlou and A. Libchaber, In Vivo Imaging of Quantum Dots Encapsulated in Phospholipid Micelles, *Science.*, 2002, **298**, 1759-1762.
- [19] J. C. Boyer, L. A. Cuccia and J. A. Capobianco, Synthesis of Colloidal Upconverting NaYF₄: Er³⁺/Yb³⁺ and Tm³⁺/Yb³⁺ Monodisperse Nanocrystals, *Nano Lett.*, 2007, **7**, 847-852.
- [20] H. R. Petty, Fluorescence Microscopy: Established and Emerging Methods, Experimental Strategies, and Applications in Immunology, *Microscopy Research and Technique.*, 2007, **70**, 687-709.
- [21] D. Q. Chen and P. Huang, Highly intense upconversion luminescence in Yb/Er: NaGdF₄@NaYF₄ core-shell nanocrystals with complete shell enclosure on core, *Dalton Trans.*, 2014, **43**, 11299-11309.
- [22] F. Wang, D. Banerjee, Y. S. Liu, X. Y. Chen and X. G. Liu, Upconversion nanoparticles in biological labeling, imaging, and therapy, *Analyst.*, 2010, **135**, 1797-2160.
- [23] M. Wang, C. C. Mi, W. X. Wang, C. H. Liu, Y. F. Wu, Z. R. Xu, C. B. Mao and S. K. Xu, Immunolabeling and NIR-Excited Fluorescent Imaging of HeLa Cells by Using NaYF₄:Yb,Er Upconversion Nanoparticles, *ACS Nano.*, 2009, **3**, 1580-1586.
- [24] L. Cheng, K. Yang, M. W. Shao, S. T. Lee and Z. Liu, Multicolor In Vivo Imaging of Upconversion Nanoparticles with Emissions Tuned by Luminescence Resonance Energy Transfer, *J. Phys. Chem. C.*, 2011, **115**, 2686-2692.
- [25] Z. Q. Li, Y. Zhang and S. Jiang, Multicolor Core/Shell-Structured Upconversion Fluorescent Nanoparticles, *Adv. Mater.*, 2008, **20**, 4765-4769.
- [26] Z. H. Chen, X. F. Wu, P. Hu, S. G. Hu, and Y. X. Liu, Multicolor upconversion NaLuF₄ fluorescent nanoprobe for plant cell imaging and detection of sodium fluorescein, *J. Mater. Chem. C.*, 2015, **3**, 153-161.
- [27] Z. H. Chen, X. F. Wu, S. G. Hu, P. Hu, H. Y. Yan, Z. J. Tang and Y. X. Liu, Upconversion NaLuF₄ fluorescent nanoprobe for jellyfish cell imaging and irritation assessment of organic dyes, *J. Mater. Chem. C.*, 2015, **3**, 6067-6076.
- [28] Y. X. Liu, D. S. Wang, J. X. Shi, Q. Peng and Y. D. Li, Magnetic Tuning of Upconversion Luminescence in Lanthanide-Doped Bifunctional Nanocrystals, *Angew. Chem. Int. Ed.*, 2013, **52**, 4366-4369.
- [29] X. C. Ye, J. E. Collins, Y. J. Kang, J. Chen, D. T. N. Chen, A. G. Yodh and C. B. Murray, Morphologically controlled synthesis of colloidal upconversion nanophosphors and their shape-directed self-assembly, *PNAS.*, 2010, **107**, 22430-22435.
- [30] J. N. Shan and Y. G. Ju, A single-step synthesis and the kinetic mechanism for monodisperse and hexagonal-phase NaYF₄:Yb, Er upconversion nanophosphors, *Nanotechnology.*, 2009, **20**, 275603-275616.

- [31] D. D. Li, Q. Y. Shao, Y. Dong and J. Q. Jiang, A facile synthesis of small-sized and monodisperse hexagonal $\text{NaYF}_4:\text{Yb}^{3+},\text{Er}^{3+}$ nanocrystals, *Chem. Commun.*, 2014, **10**, 1039-1042.
- [32] D. Yuan, M. C. Tan, R. E. Riman and G. M. Chow, A Comprehensive Study on the Size Effects of the Optical Properties of $\text{NaYF}_4:\text{Yb},\text{Er}$ Nanocrystals, *J. Phys. Chem. C.*, 2013, **117**, 13297-13304.
- [33] M. M. Lage, R. L. Moreira, F. M. Matinaga and J. Y. Gesland, Raman and Infrared Reflectivity Determination of Phonon Modes and Crystal Structure of Czochralski-Grown NaLnF_4 (Ln) La, Ce, Pr, Sm, Eu, and Gd) Single Crystals, *Chem. Mater.*, 2005, **17**, 4523-4529.
- [34] E. M. Chan, D. J. Gargas, P. J. Schuck and D. J. Milliron, Concentrating and Recycling Energy in Lanthanide Codopants for Efficient and Spectrally Pure Emission: The Case of $\text{NaYF}_4:\text{Er}^{3+}/\text{Tm}^{3+}$ Upconverting Nanocrystals, *J. Phys. Chem. B.*, 2012, **116**, 10561-10570.
- [35] F. Wang, R. Deng, J. Wang, Q. X. Wang, Y. Han, H. M. Zhu, X. Y. Chen and X. G. Liu, Tuning upconversion through energy migration in core-shell nanoparticles, *Nature. Mater.*, 2011, **10**, 968-973.
- [36] L. Pauling, The nature of the chemical bond. IV. The energy of single bonds and the relative electronegativity of atoms, *Am. Chem. Soc.*, 1932, **54**, 3570-3582.
- [37] J. N. Shan, M. J. Uddi, R. Wei, N. Yao and Y. G. Ju, The Hidden Effects of Particle Shape and Criteria for Evaluating the Upconversion Luminescence of the Lanthanide Doped Nanophosphors, *J. Phys. Chem. C.*, 2010, **114**, 2452-2461.
- [38] Y. Liu, Q. Yang, G. Ren, C. Xu and Y. Zhang, Relationship between microstructure and the achieving of the single-band red upconversion fluorescence of $\text{Er}^{3+}/\text{Yb}^{3+}$ codoped crystallites, *J. Alloys Compd.*, 2009, **467**, 351-356.
- [39] Y. Wang, F. Nan, Z. Cheng, J. Han, Z. Hao, H. Xu and Q. Wang, Strong tunability of cooperative energy transfer in Mn^{2+} -doped ($\text{Yb}^{3+}, \text{Er}^{3+}$)/ NaYF_4 nanocrystals by coupling with silver nanorod array, *Nano Research.*, 2015, **8**, 2970-2977.
- [40] S. Fang, C. Wang, J. Xiang, L. Cheng, X. Song, L. Xu, R. Peng and Z. Liu, Aptamer-conjugated upconversion nanoprobe assisted by magnetic separation for effective isolation and sensitive detection of circulating tumor cells, *Nano Research.*, 2014, **7**, 1327-1336.
- [41] J. C. Boyer, L. A. Cuccia and J. A. Capobianco, Synthesis of Colloidal Upconverting $\text{NaYF}_4:\text{Er}^{3+}/\text{Yb}^{3+}$ and $\text{Tm}^{3+}/\text{Yb}^{3+}$ Monodisperse Nanocrystals, *Nano Lett.*, 2007, **7**, 848-852.



It can be addressed based on luminescence resonant energy transfer (LRET) technology that no Rhodamine B is absorbed by fishes after incubating in the aqueous solution of 1 $\mu\text{g/ml}$ Rhodamine B for one day, while sodium fluorescein residue can be obviously detected after incubating in the aqueous solution of 1 $\mu\text{g/ml}$ sodium fluorescein for one day.